Anal Bioanal Chem (2012) 404:3145–3154
DOI 10.1007/s00216-012-6434-4

ORIGINAL PAPER

UPLC-UV-MS^E analysis for quantification and identification of major carotenoid and chlorophyll species in algae

Weiqi Fu · Manuela Magnúsdóttir · Sigurður Brynjólfson · Bernhard Ø. Palsson · Giuseppe Paglia

Received: 19 August 2012 / Revised: 14 September 2012 / Accepted: 18 September 2012 / Published online: 2 October 2012

Abstract A fast method for quantification and identification of carotenoid and chlorophyll species utilizing liquid chromatography coupled with UV detection and mass spectrometry has been demonstrated and validated for the analysis of algae samples. This method allows quantification of targeted pigments and identification of unexpected compounds, providing isomers separation, UV detection, accurate mass measurements, and study of fragment ions for structural elucidation in a single run. This is possible using parallel alternating low- and high-energy collision spectral acquisition modes, which provide accurate mass full scan chromatograms and accurate mass high-energy chromatograms. Here, it is shown how this approach can be used to confirm carotenoid and chlorophyll species by identification of key diagnostic fragmentations during high-energy mode. The developed method was successfully applied for the analysis of *Dunaliella salina* samples during defined red LED lighting growth conditions, identifying 37 pigments including 19 carotenoid species and 18 chlorophyll species, and providing quantification of 7 targeted compounds. Limit of detections for targeted pigments ranged from 0.01 ng/mL for lutein to 0.24 ng/mL for chlorophyll *a*. Inter-run precision ranged for of 3 to 24 (RSD%) while inter-run inaccuracy ranged from −17 to 11.

Keywords Carotenoids · Chlorophylls · UPLC · Mass spectrometry · MS^E · *Dunaliella salina*

Introduction

Carotenoids and chlorophylls are the major pigment species in higher plants and algae. Chlorophylls are Mg^{2+}-porphyrins, and are the most abundant tetrapyrrole molecules in plants, being involved in photosynthetic light-harvesting and energy transduction as well as in reaction center (e.g., photosystem II) [1].

Carotenoids, including both carotenes and xanthophylls, such as β-carotene and lutein, play a central role in the photosystem II protecting the photosynthetic apparatus against photo-oxidative damage by deactivation of reactive oxygen species (ROS) and reduction of ROS formation under excess light in higher plants as well as in green algae [2, 3].

Carotenoids are broadly distributed in both phototrophic and non-phototrophic organisms, and are extremely important for nutritional purposes of human beings [4–6].

They belong to a group of red and yellow pigments with light absorption between 450 and 570 nm in the visible light range and in natural sources they occur mainly in the all-*trans* configuration [7]. The *trans* to *cis* isomerization mainly occurs in stressful conditions such as light exposure or heat treatment [7]. However, 9-*cis* β-carotene and phytoene are also presented in plants such as *Dunaliella bardawil* under lower or natural light conditions [8].

Identification and quantification of carotenoid and chlorophyll species is fundamental in nutritional and metabolic engineering sciences. For instance, by using adaptive laboratory evolution [9], it might be possible to improve strain

Electronic supplementary material The online version of this article (doi:10.1007/s00216-012-6434-4) contains supplementary material, which is available to authorized users.

W. Fu · M. Magnúsdóttir · S. Brynjólfson · B. Ø. Palsson · G. Paglia (✉)
Center for Systems Biology, University of Iceland,
Sturlugata 8,
IS 101 Reykjavik, Iceland
e-mail: gpaglia@hi.is

performance in microalgal biotechnology with the scope of increasing yields of carotenoids. In this scenario, understanding the effect of light conditions on algae is fundamental, and it requires high-throughput procedures for the identification and the quantification of pigments.

Conventional methods for quantification of pigments rely mainly on HPLC-UV methods [8, 10–12]. Most recently, several papers have been presented coupling HPLC-DAD with mass spectrometry (MS). These strategies, using time-of-flight (TOF) [13–16] or triple quadrupole (QqQ) [17–19] as MS detector, allow identification of higher number of pigments. Nevertheless, MS strategies for metabolite identification are usually time-consuming. In fact, in the case of QqQ-MS detection, additional fragmentation studies are needed for optimization of MS/MS conditions, which requires availability of pure standards or preliminary identification of pigments presents in the sample [17]. On the other hand, TOF-MS detection provides exact mass measurements but still requires further fragmentation studies to confirm tentatively identified metabolites.

In recent years, UPLC-MS^E analysis (where E represents collision energy) has been proposed as unbiased strategy to shorten time of analysis, collecting both unfragmented and fragmented ions, which consecutively can be used for quantification and fragment-ion information [20, 21]. MS^E analysis simultaneously provides exact mass measurements and fragmentation information by collecting data using parallel alternating low- and high-energy collision spectral acquisition modes and can be used as an alternative approach to data-dependent MS/MS mode.

This approach has been successfully used for lipid analysis [21, 22] and for characterization of the biotransformation products of drug candidates [23].

The aim of this work was to develop a method for quantification of targeted pigments and identification of unexpected compounds in algae samples. This was achieved by using a UPLC-UV-MS^E method, which, in a single 20-min analysis, provides isomers separation, UV detection, accurate mass measurements and MS/MS spectra for structural elucidation. Performances of the presented method were tested for analysis of carotenoid and chlorophyll species in *Dunaliella salina* samples during defined red LED lighting growth conditions.

Materials and methods

Chemicals and materials

All materials were obtained from Sigma-Aldrich (Seelze, Germany) unless stated otherwise. Acetonitrile was purchased from Merck (Darmstadt, Germany). Water was obtained using an 18 Ωm Milli-Q (Millipore, USA). Lutein, β-carotene, zeaxanthin, lycopene, chlorophyll *a*, and chlorophyll *b* were purchased from Sigma-Aldrich (Seelze, Germany).

α-Carotene was obtained from Santa Cruz Biotechnology (Santa Cruz, CA, USA).

All chemicals and solvents were of analytical grade or higher purity.

Microalga and growth conditions

D. salina was purchased from the University of Texas (UTEX LB #200) and grown in Gg-8 medium (see Electronic supplementary material (ESM), Table S2) by modifying Gg medium (11) at 25±2 °C. Bubble column photobioreactors were cylindrical with H=30 cm, D= 4 cm, and a working volume of 300±5 ml. Input gas was 90 ml/min of 2.5 % CO_2 in air. Culture pH was regulated between 6.5 and 7.5. *D. salina* cells were grown under lower light intensity (e.g., 85 μE/m^2/s) of red LED lighting (peak at 660 nm with narrow spectra) for 5 days.

Sample treatment

A 0.5-ml aliquot of cell suspension was centrifuged at 1,000×*g* for 10 min. The pellet containing the cells was then extracted with 3 ml of ethanol/hexane 2:1 (*v*/*v*) containing 0.1 % (*w*/*v*) butylated hydroxytoluene [17, 24]. Two milliliters of water and 4 ml of hexane were added and the mixture was vigorously shaken and centrifuged again at 1,000×*g* for 5 min. The hexane layer (upper layer) was separated and an aliquot (4 ml) of this extract was evaporated under N_2 at 25±2 °C, reconstituted in methyl tertiary butyl ether + acetonitrile (MTBE + ACN) (50+50, *v* + *v*) and 5 μL were injected in the UPLC system analyzed by UPLC-UV-MS^E.

Liquid chromatography and UV detection

UPLC separation was performed on an ACQUITY UPLC (Waters, MS Technologies, UK) in reversed-phase chromatography using an ACQUITY UPLC HSS T3 1.8 μm (2.1× 150 mm) column (Waters, Manchester, UK). The mobile phase was designed as phase A, consisting of a mixture of ACN + methanol (MeOH) + MTBE (70+20+10, *v* + *v* + *v*) (A) and phase B 10 mM ammonium acetate (B). Column temperature was 45 °C and the elution flow rate was 0.5 mL/min with a gradient: 60 % mobile phase A at 0 min, 75 % A at 4 min, 100 % A at 12 min, 98 % A 15 min and 60 % A between 16 and 20 min.

A TUV detector (Waters, MS technologies, UK) was used for UV detection at 450 nm.

Mass spectrometry

The inlet (UPLC-UV system) was coupled in line with a quadrupole–time-of-flight hybrid mass spectrometer (Synapt G2, Waters, Manchester, UK), using electrospray ionization interface (positive mode) to direct column eluent to the mass spectrometer.

The mass spectrometer operated in V mode for high sensitivity using a capillary voltage of 3 kV and a cone voltage of 30 V. Cone and desolvation gas flow was 20 and 800 L/h, respectively, while source and desolvation gas temperature was 100 and 500 °C, respectively. Leucine enkephalin (2 ng/μL) was used as lock mass (*m*/*z* 556.2771).

Data were acquired in MS^E mode from *m*/*z* 50 to 1000, creating two discrete and independent interleaved acquisition functions. The first acquisition, set at 5 eV of collision energy, collects low energy of unfragmented data, while the second has a collision energy ramp from 20–30 eV and collects fragmented data. Argon was used for collision-induced dissociation.

MS^E data viewer (Waters, Manchester, UK) was used for visualization and alignment of low- and high-energy information.

MarkerLynx (Waters, Manchester, UK) was used to integrate and align MS data points and to convert them into exact mass retention time pairs.

QuanLynx (Waters, Manchester, UK) was used to integrate chromatograms of tentatively identified metabolites.

Results and discussion

UPLC-UV-TOF-MS^E analysis

To understand the effect of light conditions on algae it becomes important to identify and quantify carotenoids and chlorophyll species in their respective molecular classes. In order to achieve this objective, we developed a method able to quantify targeted compounds and identify untargeted metabolites using an UPLC-UV-TOF-MS^E approach. This strategy provides simultaneously, isomers

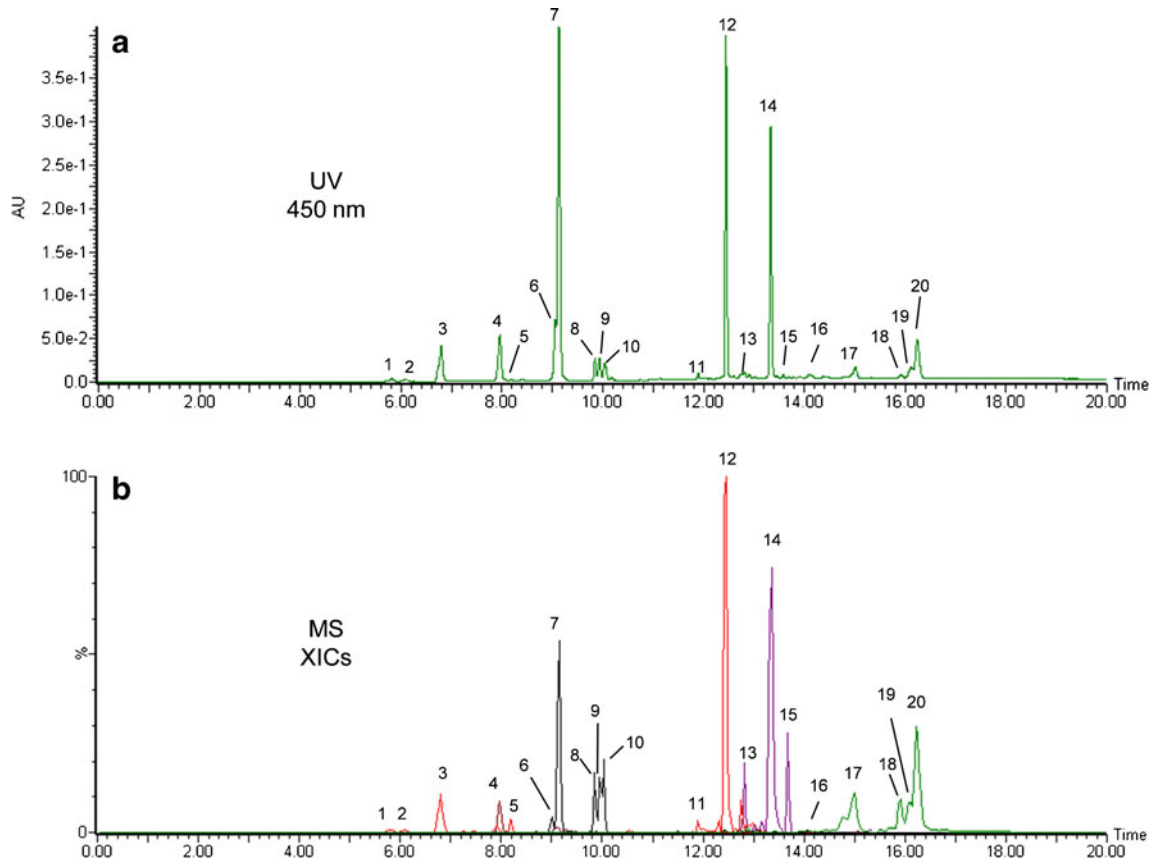

Fig. 1 UV and MS chromatograms from a *D. salina* sample cultured as described in the "Materials and methods". **a** UV detection at 450 nm. **b** Overlaid extracted ion chromatograms (XICs) obtained in positive mode ESI-MS detection. (*1*) Neoxanthin, (*2*) neoxanthin isomer, (*3*) violaxanthin, (*4*) antheraxanthin, (*5*) violaxanthin isomer, (*6*) zeaxanthin, (*7*) lutein, (*8*) lutein isomer, (*9*) lutein isomer, (*10*) lutein isomer, (*11*) chlorophyll *b* derivatives, (*12*) chlorophyll *b*, (*13*) chlorophyll *a* derivatives, (*14*) chlorophyll *a*, (*15*) chlorophyll *a*′, (*16*) lycopene, (*17*) δ-carotene, (*18*) α-carotene, (*19*) *cis*-β-carotene, (*20*) *trans*-β-carotene

separation, UV detection, accurate mass measurements, and MS/MS spectra for structural elucidation.

Carotenoids have been traditionally separated using reverse-phase chromatography using specific C30 columns [10]. These approaches are usually time-consuming; nevertheless, the complexity and the higher number of isomeric carotenoid species require efficient separation in order to achieve correct species identification.

The use of ion mobility-MS was also investigated to resolve and separate geometrical carotenoid isomers. This task was only partially achieved because of the high source temperature, which causes *cis*/*trans* isomerization in the ESI source [25].

Chauveau-Duriot et al. presented an UPLC-UV separation with a C18 column providing separation of main carotenoid species with a 45-min run [26]. We used the same HSS T3 column to develop a 20-min UPLC-UV-MS method that is well suited for identification of major carotenoids and chlorophyll species. The chromatographic elution was designed in order to provide separation of both xanthophylls and carotenes isomers in a reasonable time of analysis. Carotenoids isomers are usually difficult to resolve, moreover they have a wide range of polarity, ranged from the more polar xanthophylls to carotenes. For this reason, a HSS T3 column was chosen since it provides efficient retention and separation of polar compounds [26].

In this method, xanthophyll isomers are eluted at lower retention times and are resolved as shown in Fig. 1, achieving separation of different isomers of violaxanthin and lutein.

Carotenes elute at higher retention times, achieving separation of lycopene, δ-carotene, α-carotene and β-carotene, while separation of *trans* and *cis*-β-carotene, was only partially achieved (Fig. 1).

UPLC-UV-MS detection yields to a first set of information for the identification of these pigments; nevertheless, for unambiguous identification, the approach developed provides a further dimension consisting of the study of fragmentation products.

In fact, UPLC-MS^E detection collects data using two scan functions resulting in two different mass chromatograms. In the first function (low energy), the first quadrupole (Q1) scanned *m*/*z* 50–1,000 and transmission of intact ions through the collision cell is achieved by using low collision energy (5 eV). These ions are

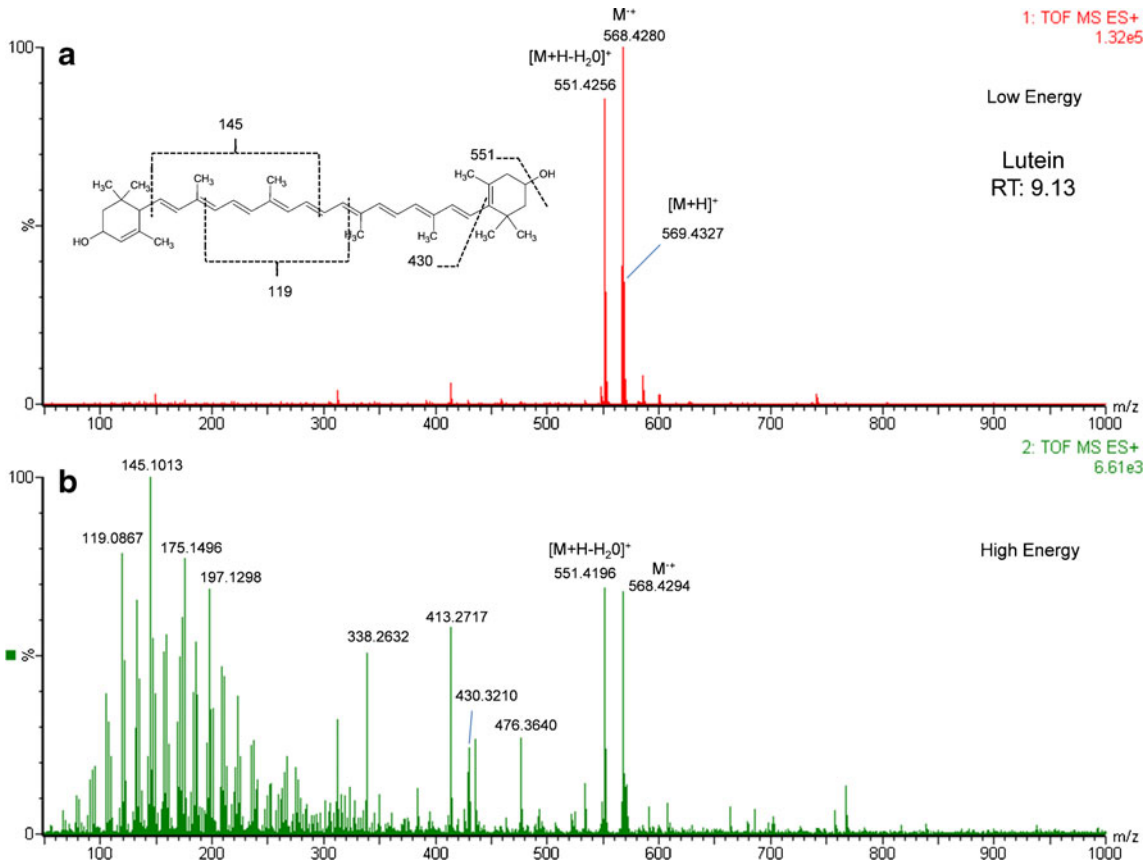

Fig. 2 Lutein identification in a *D. salina* sample cultured as described in the "Materials and methods". **a** Low-energy spectrum (5 eV) of lutein obtained from a real sample. **b** High-energy spectrum (20–30 eV) of lutein obtained from a real sample

pushed into the TOF analyzer for exact mass measurements. The low-energy function provides information on intact molecules. The second function (high energy) scanned the same mass range in the Q1, while in the collision cell the high collision energy (20–30 eV) fragments all the ions transmitted by Q1. The high-energy function provides information of fragments and can be used as an alternative approach to data-dependent MS/MS mode.

Identification of carotenoids

In our experiments, carotenoid species shown as base peaks, protonated molecules $[M+H]^+$ and/or a radical ions $M^{\cdot+}$ (see ESM, Table S1). For instance, in Fig. 2 is shown the low- and high- energy spectra of lutein, detected at retention time of 9.13 min. In the low-energy spectrum, lutein shows three peaks, the protonated molecule $[M+H]^+$ at *m/z* 569.4327, the radical ion $M^{\cdot+}$ at *m/z* 568.4280 and the ion at *m/z* 551.4256 which corresponds to the loss of one molecule of water (Fig. 2a). Further confirmation of lutein was provided by the high-energy function, which gives a spectrum resulting from fragmentation of all three ions listed above (Fig. 2b).

Figure 3 shows low- and high-energy spectrum of the signal detected at retention time of 7.97 min tentatively identified as antheraxanthin. The low-energy spectrum shows a base peak at *m/z* 585.4294 that corresponds to the protonated molecule (Fig. 3a) while its fragment ions are shown in the high-energy spectrum (Fig. 3b), allowing confirmation of antheraxanthin.

In this way, ions detected in low-energy modes that had absorbance at 450 nm and molecular masses matching with carotenoid species were confirmed by using fragmented ions information obtained in high-energy modes. Further examples relative to carotenes are shown in Figure S1 of the ESM.

High-energy modes can also be used to identify key diagnostic fragmentation. For example, in Fig. 4, it is shown how violaxanthin and neoxanthin isomers can be confirmed by identification of a fragment ion in common. Low-energy mass spectrum at 6.78 min shows two ions at *m/z* 601.4218 and *m/z* 583.4005 which are the protonated violaxanthin and the ion corresponding to the loss of a molecule of water (Fig. 4c). The high-energy

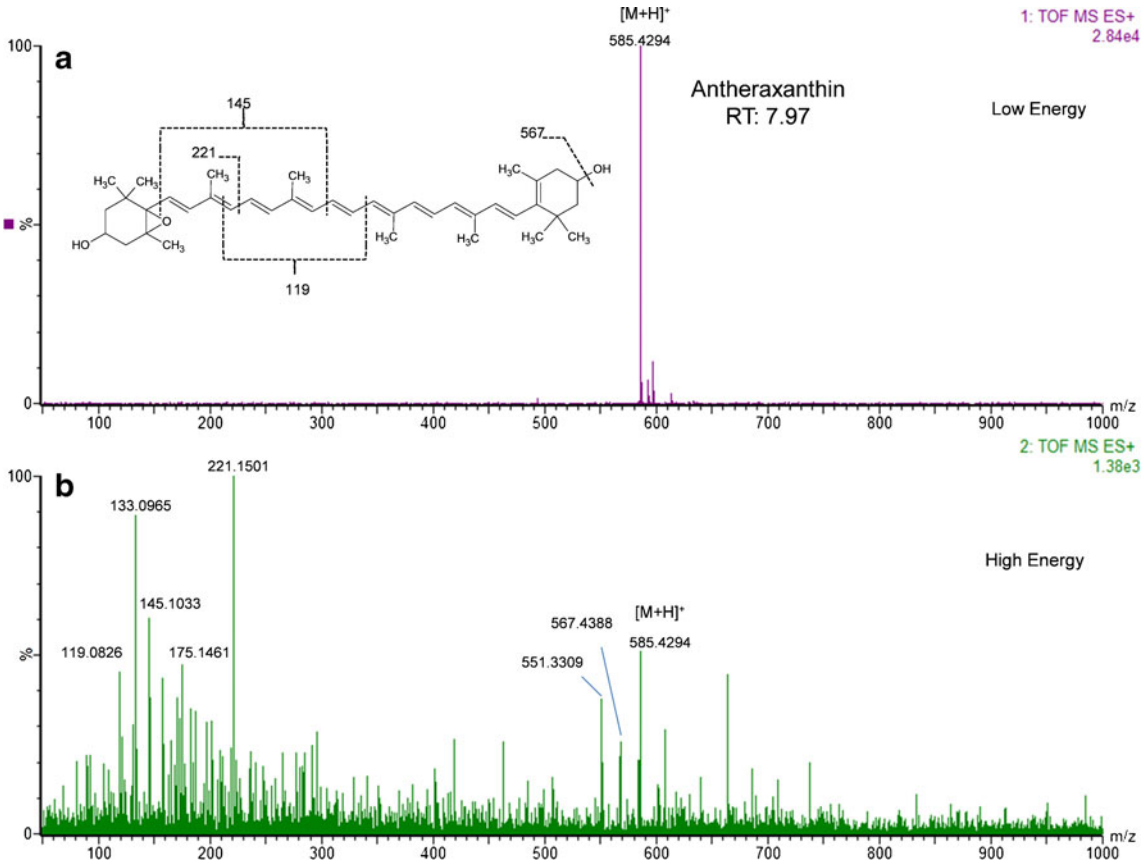

Fig. 3 Antheraxanthin identification in a *D. salina* samples cultured as described in the "Materials and methods". **a** Low-energy spectrum (5 eV) of antheraxanthin obtained from a real sample. **b** High-energy spectrum (20–30 eV) of antheraxanthin obtained from a real sample

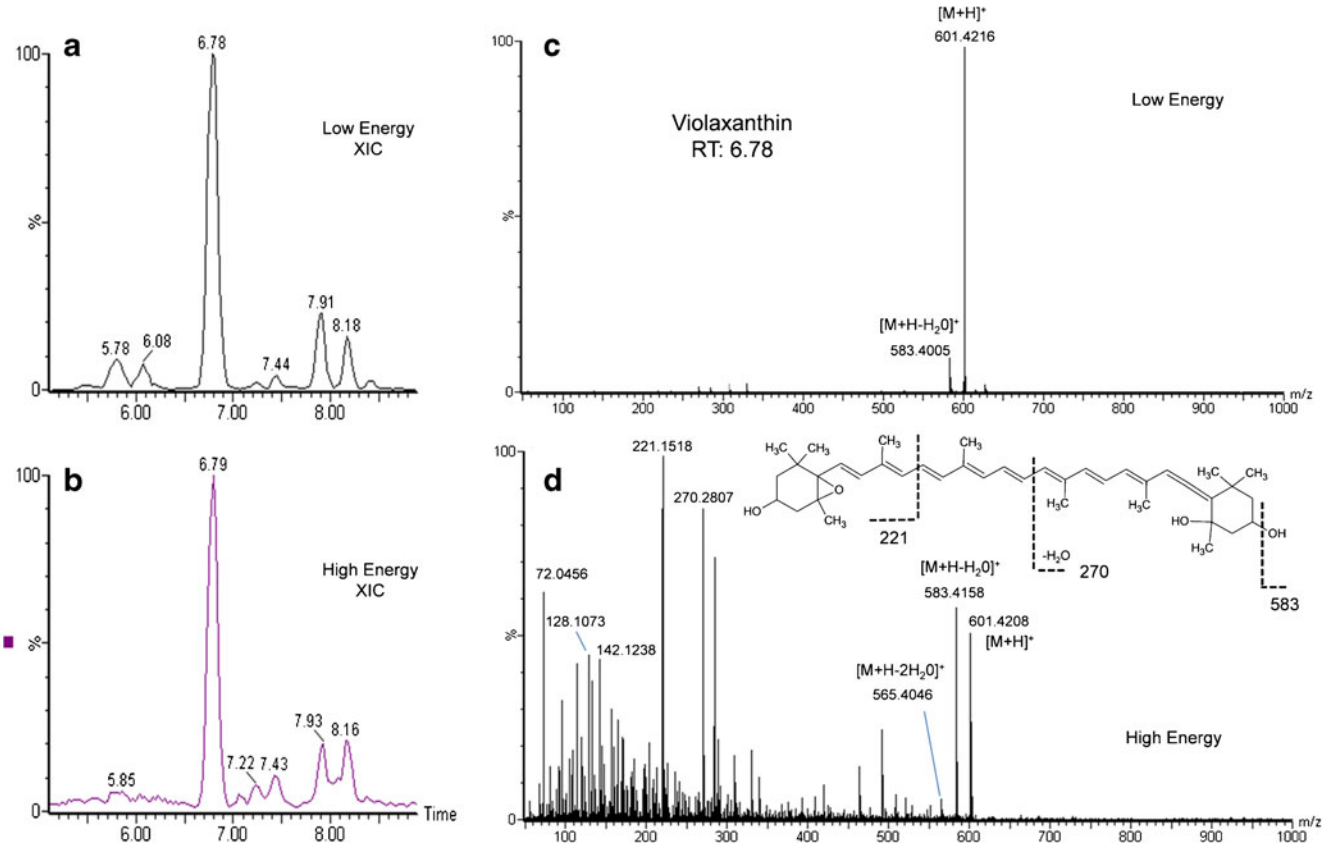

Fig. 4 Violaxanthin identification in a *D. salina* sample cultured as described in the "Materials and methods". **a** Low-energy XIC of 601.4216. **b** High-energy XIC of 221.1518. **c** Low-energy spectrum at 6.78 min. **d** High-energy spectrum at 6.78 min for violaxanthin identification

mass spectrum instead shows fragments of violaxanthin, pointing out a fragment at *m/z* 221.1518 which can be used as fragment ion for confirmation of other isomers. This ion results to the cleavage of the single bond C10–C11 (Fig. 4d) and it is a common fragment between violaxanthin and neoxanthin isomers. In fact, extracted ion chromatogram (XIC) of the ion at *m/z* 601.422 in low-energy mode provides six peaks (Fig. 4a) and these peaks overlapped with the ones obtained in the high energy from XIC of the ion at *m/z* 221.152 (Fig. 4b). These chromatographic peaks were identified as violaxanthin and its isomers (see ESM, Table S1).

Exact mass measurements and fragmentation data provided by MS^E strategy led to identification of 19 different carotenoid species in *D. salina* samples (see ESM, Table S1).

Identification of chlorophylls

Chlorophylls are a group of tetrapyrrole pigments involved in light reactions of photosynthesis. The two main species are chlorophyll *a* and *b*. In Fig. 1, combining MS and UV detection, two intense peaks were detected for chlorophyll *a* (13.35 min) and *b* (12.44 min). However, other chlorophyll species can be detected in algae samples and in this work, we used high-energy functions and key diagnostic fragmentations of chlorophyll pigments to identify unexpected species.

In Fig. 5d is shown the high-energy spectrum of chlorophyll *b*. Fragmentation of chlorophyll *b* provides three main fragments, which are a consequence of the loss of phytyl or phytyl ester chain. At *m/z* 629.2240 was detected the fragment identified as $[M\text{-}C_{20}H_{38}+H]^+$, at *m/z* 569.2036 we assigned a fragment due to the loss of phytyl ester chain (M-CH_2COO-phytyl) corresponding to $[M\text{-}C_{22}H_{41}O_2]^+$. Finally, the fragment at *m/z* 597.1985 was attributed to $[M\text{-}C_{20}H_{38}O_2+H]^+$.

It was interesting to notice that a similar fragmentation pattern was observed for other compounds showing absorption at 450 nm (Fig. 5c); in fact, as shown in Fig. 5e, fragmentation of the ion at *m/z* 905.5068 detected at 11.77 min yields to the same three fragment ions of chlorophyll *b*. This behavior suggests a compound with the same tetrapyrrole ring but different phytyl chain. We assigned to this chlorophyll species a molecular formula of $C_{55}H_{68}MgN_4O_6$ with two double

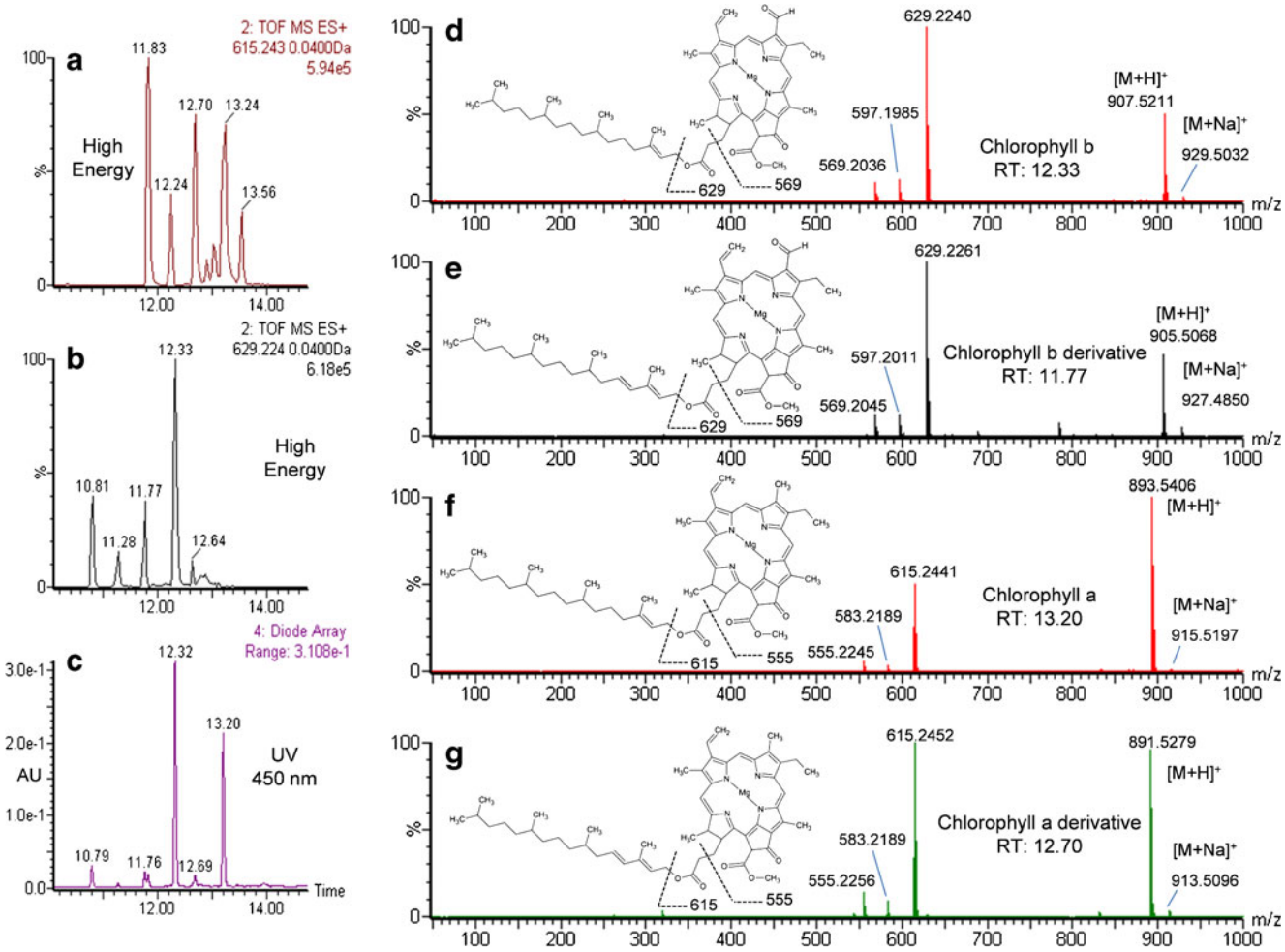

Fig. 5 Chlorophyll species identification in a *D. salina* sample cultured as described in the "Materials and methods". **a** High-energy XIC of 615.243 for identification of chlorophyll *a* derivatives. **b** High-energy XIC of 629.224 for identification of chlorophyll *b* derivatives. **c** UV chromatogram at 450 nm. **d** High-energy spectra at 12.33 min for identification of chlorophyll *b*. **e** High-energy spectra at 11.77 min for identification of chlorophyll *b* derivative. **f** High-energy spectra at 13.20 min for identification of chlorophyll *a*. **g** High-energy spectra at 12.70 min for identification of chlorophyll *a* derivative

bonds (C═C) on the phytyl chain. Since chlorophyll *b* and its derivative have these three fragments in common, we can use them to search and identify other chlorophyll species. In fact, as shown in Fig. 5b, high-energy XIC at *m/z* 629.2240 extracted five different peaks.

Examination of the high-energy spectra demonstrates that all these ions exhibit the same fragmentation pattern, allowing identification of chlorophyll *b*' and other two derivative species at *m/z* 903.4916 ($C_{55}H_{66}MgN_4O_6$) and 901.4763 ($C_{55}H_{64}MgN_4O_6$) with three and four unsaturations (C═C) on the phytyl chain (see ESM, Figure S2, Table S1).

Chlorophyll *a* differs from chlorophyll *b* as it contains a methyl group instead of an aldehyde on the tetrapyrrole ring. This group gives chlorophyll *a* less polar characteristic and for these reasons it is more retained during RPLC. As seen in Fig. 5f, chlorophyll *a* shows the same fragmentation pattern that leads to the loss of phytyl chain, $[M\text{-}C_{20}H_{38}+H]^+$ at *m/z* 615.2441, loss of phytyl ester chain (M-CH_2COO-phytyl) at *m/z* 555.2245, and finally the fragment at *m/z* 583.2189 $[M\text{-}C_{20}H_{38}O_2+H]^+$. Even for chlorophyll *a*, the fragment ion at *m/z* 615.2441 can be used as precursor ion to extract from the high-energy mass chromatogram species having same fragmentation pattern. In fact, in Fig. 5a, the XIC at *m/z* 615.244 presents several peaks that were identified as chlorophyll derivatives (see ESM, Figure S3 and Table S1). For instance, at 12.70 min, the ion at *m/z* 891.5279 was tentatively identified as a chlorophyll *a* derivative with a molecular formula of $C_{55}H_{70}MgN_4O_5$, its high-energy spectrum (Fig. 5g) provides the same three main fragment ions of chlorophyll *a*, suggesting a chlorophyll *a* derivative with two double bonds (C═C) on the phytyl chain.

Table 1 Calibration curve, linear range, and limit of detection

Compound	Slope ± SD (n=4)	Intercept ± SD (n=4)	R^2±SD (n=4)	Linear range (μg/mL)	RSD% lowest point (n=12)	Lod ± SD (ng/mL) (n=12)
trans-β-Carotene	2015.5 s±90.2	135.2±4.1	0.9995±0.0004	0.06–30	9.3	0.033±0.004
α-Carotene	5961.2±179.1	37.1±6.2	0.9993±0.0005	0.0078–4	6.3	0.011±0.001
Lycopene	3496.9±124.5	117.7±3.9	0.9971±0.0016	0.0078–4	10.5	0.031±0.005
Zeaxanthin	4026.0±172.0	222.7±27.71	0.9915±0.0008	0.0078–4	8.7	0.021±0.004
Lutein	5095.2±211.3	326.8±38.4	0.9990±0.0006	0.4–20	5.4	0.010±0.001
Chlorophyll *b*	2945.6±81.5	683.4±53.3	0.9978±0.0021	0.078–40	6.7	0.018±0.002
Chlorophyll *a*	157.39±12.3	44.1±11.3	0.9992±0.0007	0.2–80	11.8	0.24±0.001

Chlorophyll *a*′ and other two chlorophyll *a* derivatives were also identified in this way (see ESM, Table S1), and the high-energy spectra are shown in Figure S3 of the ESM.

Pheophytin *a* and *b* were also detected in algae samples and the same strategy was used to identify pheophytin derivative species (see ESM, Figure S4 and Table S1). Pheophytins are Mg-free chlorophylls playing a role as electron intermediates in the electron transfer pathway of photosystem II. Due to the similar structure, it is reasonable to assume that they possess a similar fragmentation pattern of chlorophyll. In fact, in Figure S4 (see ESM) are shown the high-energy spectra of ions at *m*/*z* 869.5549, *m*/*z* 871.5730, and *m*/*z* 871.5728. These three ions showed a fragment in common at *m*/*z* 593.276 that corresponds to loss of phytyl chain. In this way, pheophytin *a*, pheophytin *a*′ and pheophytin *a* derivative were identified (see ESM, Table S1 and Figure S4).

Quantitative analysis

The presented method was designed for quantification of targeted compounds and identification of unexpected metabolites. Seven targeted compounds were selected and quantification was achieved by the use of their corresponding pure standards (Table 1). Quantitative analysis was achieved using UV detection except for zeaxanthin. For zeaxanthin, MS detection was chosen due to its better separation from lutein. Limits of detection (Lods) were calculated as the quantity of analyte able to produce a chromatographic peak three times higher than the noise (S/N=3) in a non-fortified sample after estimation of endogenous concentration. Lods ranged from 0.01 ng/mL for lutein to 0.24 ng/mL for chlorophyll *a* (Table 1). The higher limit of detection of chlorophyll *a* is due to the UV detection at

Table 2 Intra- and inter-run precision and inaccuracy

Metabolite	QC (μg/mL)	Intra-run						Inter-run	
		Day 1		Day 2		Day 3		Inaccuracy	RSD%
		Inaccuracy	RSD %	Inaccuracy	RSD %	Inaccuracy	RSD %		
trans-β-Carotene	2.1	−3	3	−4	5	−19	4	−16	5
	11.4	−17	5	−17	6	6	7	−4	9
Zeaxanthin	0.8	1	10	11	33	20	13	11	8
	1.5	−6	18	−19	20	10	1	−5	10
Lutein	5.6	−9	8	8	9	7	6	2	9
	8.9	−12	10	2	11	0	12	−3	8
Chlorophyll *a*	41.6	−3	9	2	11	7	6	1	12
	65.0	−5	12	−14	4	−2	5	−4	3
Chlorophyll *b*	7.4	−13	8	6	10	3	2	−1	11
	30.7	−18	3	−12	6	27	8	−1	24
α-Carotene	0.8	−10	13	−16	10	−18	4	−17	1
	1.4	−18	8	−17	8	20	3	−5	23
Lycopene	0.7	11	10	13	12	−17	4	5	18
	1.4	−2	11	3	15	−10	3	0	9

450 nm. In fact, chlorophyll has a max absorbance at 680 nm. Nevertheless, concentration of chlorophyll *a* in *D. salina* samples is at least 1,000 times higher than its Lod.

Reproducibility and accuracy were investigated using quality control (QC) samples fortified with known amount of standards. Intra-run precision was calculated as relative standard deviation (RSD%) for two QC at different concentrations. During analysis of three batches, the RSD% was higher than 20 just in one case—for zeaxanthin at the lowest concentration (Table 2). Inter-run precision ranged 3 to 24 for RSD% (Table 2). Zeaxanthin shows some relatively large RSD% (higher than 20) (Table 2). This might be due to the matrix effect considering that MS detection was used for this compound.

Intra-run inaccuracy was higher than ±20 just in one case and inter-run inaccuracy ranged from −17 to 11 (Table 2).

Carotenoid and chlorophyll species analysis in *D. salina*

The presented method was used for quantification and identification of pigments in *D. salina* samples. The growth profile of *D. salina* under lower light intensity (e.g., 85 μE/m^2/s photon flux of red light) could be regarded as light-dependent growth in batch culture with the following equation: $C_T = aT + C_0$, where C_T stands for the biomass concentration (gram dry cell weight per liter, gDCW/L), a for the linear growth coefficient (gDCW/L/day), T for the cultivation time (day), and C_0 for the initial biomass concentration (gDCW/L). In this case, a was calculated as 0.17 gDCW/L/day (R^2= 0.99) based on three independent experiments. In these samples, 37 different pigments were detected. The contents of β-carotene, lutein, lycopene (the precursor of both β-carotene and lutein), and zeaxanthin (the first downstream metabolite of β-carotene) were analyzed under the stated red LED lighting condition. Among all detected pigments in *D. salina* cells, all-*trans*-β-carotene and lutein are major pigments in addition to chlorophylls (Fig. 6). The results indicated that the total content of these four carotenoids would reach its maximum level in 5 days of culture (Fig. 6). It appeared that light stress-induced carotenoids accumulation in *D. salina* over time and achieved a relatively stable level ultimately. Further, we found that the major carotenoids changed in parallel to the chlorophyll *b* (Fig. 6b) though the ratio of the major carotenoids to chlorophyll *b* content was varied over time.

These results characterize major carotenoids and chlorophylls accumulated in *D. salina* under red light conditions and provide the grounds for understanding major pigments metabolism in green algae.

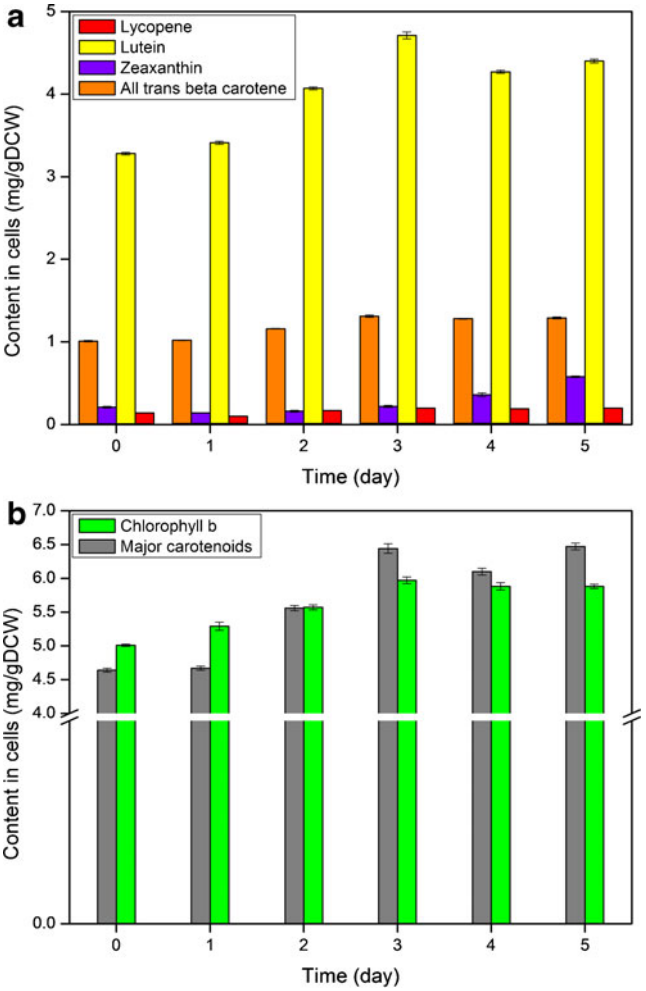

Fig. 6 Pigments accumulation in *D. salina* in batch culture. **a** Lycopene, *trans*-β-carotene, lutein, and zeaxanthin content. **b** Major carotenoids (the sum of four stated carotenoids) and chlorophyll *b* content. The results are averaged from three independent experiments. *Error bars* indicate SD

Conclusion

We developed an UPLC-UV-MS^E method for major carotenoids and chlorophyll species analysis, which provides, in a single run, isomers separation, UV detection, accurate mass measurements, and MS/MS spectra for structural elucidation.

We have demonstrated that this method can be used to quantify targeted pigments and to identify and confirm unexpected compounds combining information coming from unfragmented and fragmented data by the use of key diagnostic fragmentations.

The method was tested by analyzing *D. salina* samples during defined red LED lighting growth conditions, identifying 37 pigments species including 19 carotenoid species and 18 chlorophyll species, and providing quantification of 7 targeted compounds.

These results demonstrated that this method is suitable for high-throughput analysis of pigments in complex matrices as algae samples.

Acknowledgments The Icelandic Technology Development Fund supported this research.

References

1. Reinbothe S, Reinbothe C (1996) The regulation of enzymes involved in chlorophyll biosynthesis. Eur J Biochem 237(2):323–343
2. Telfer A (2002) What is beta-carotene doing in the photosystem II reaction centre? Philos Trans R Soc B-Biol Sci 357(1426):1431–1439. doi:10.1098/rstb.2002.1139, discussion 1439–1440, 1469–1470
3. Jahns P, Holzwarth AR (2012) The role of the xanthophyll cycle and of lutein in photoprotection of photosystem II. Biochim Biophys Acta 1817(1):182–193. doi:10.1016/j.bbabio.2011.04.012
4. Takaichi S (2011) Carotenoids in algae: distributions, biosyntheses and functions. Mar Drugs 9(6):1101–1118. doi:10.3390/md9061101
5. Carpentier S, Knaus M, Suh M (2009) Associations between lutein, zeaxanthin, and age-related macular degeneration: an overview. Crit Rev Food Sci Nutr 49(4):313–326. doi:10.1080/10408390802066979
6. Darvin ME, Fluhr JW, Meinke MC, Zastrow L, Sterry W, Lademann J (2011) Topical beta-carotene protects against infra-red-light-induced free radicals. Exp Dermatol 20 (2):125–129. doi:10.1111/j.1600-0625.2010.01191.x
7. Kamffer Z, Bindon KA, Oberholster A (2010) Optimization of a method for the extraction and quantification of carotenoids and chlorophylls during ripening in grape berries (*Vitis vinifera* cv. Merlot). J Agric Food Chem 58(11):6578–6586. doi:10.1021/jf1004308
8. Ben-Amotz A, Lers A, Avron M (1988) Stereoisomers of beta-carotene and phytoene in the alga *Dunaliella bardawil*. Plant Physiol 86(4):1286–1291
9. Palsson BO (2011) Adaptive laboratory evolution. Microbe 6 (2):69–74
10. Bino RJ, Ric de Vos CH, Lieberman M, Hall RD, Bovy A, Jonker HH, Tikunov Y, Lommen A, Moco S, Levin I (2005) The light-hyperresponsive high pigment-2dg mutation of tomato: alterations in the fruit metabolome. New Phytol 166(2):427–438. doi:10.1111/j.1469-8137.2005.01362.x
11. Moco S, Capanoglu E, Tikunov Y, Bino RJ, Boyacioglu D, Hall RD, Vervoort J, De Vos RC (2007) Tissue specialization at the metabolite level is perceived during the development of tomato fruit. J Exp Bot 58(15–16):4131–4146. doi:10.1093/jxb/erm271
12. Pott I, Marx M, Neidhart S, Muhlbauer W, Carle R (2003) Quantitative determination of beta-carotene stereoisomers in fresh, dried, and solar-dried mangoes (*Mangifera indica* L.). J Agric Food Chem 51(16):4527–4531. doi:10.1021/jf034084h
13. Ranga Rao A, Raghunath Reddy RL, Baskaran V, Sarada R, Ravishankar GA (2010) Characterization of microalgal carotenoids by mass spectrometry and their bioavailability and antioxidant properties elucidated in rat model. J Agric Food Chem 58 (15):8553–8559. doi:10.1021/jf101187k
14. Ranga R, Sarada AR, Baskaran V, Ravishankar GA (2009) Identification of carotenoids from green alga *Haematococcus pluvialis* by HPLC and LC-MS (APCI) and their antioxidant properties. J Microbiol Biotechnol 19(11):1333–1341
15. Ornelas-Paz Jde J, Yahia EM, Gardea-Bejar A (2007) Identification and quantification of xanthophyll esters, carotenes, and tocopherols in the fruit of seven Mexican mango cultivars by liquid chromatography-atmospheric pressure chemical ionization-time-of-flight mass spectrometry [LC-(APcI(+))-MS]. J Agric Food Chem 55(16):6628–6635. doi:10.1021/jf0706981
16. Aparicio-Ruiz R, Riedl KM, Schwartz SJ (2011) Identification and quantification of metallo-chlorophyll complexes in bright green table olives by high-performance liquid chromatrography-mass spectrometry quadrupole/time-of-flight. J Agric Food Chem 59 (20):11100–11108. doi:10.1021/jf201643s
17. Gentili A, Caretti F (2011) Evaluation of a method based on liquid chromatography-diode array detector-tandem mass spectrometry for a rapid and comprehensive characterization of the fat-soluble vitamin and carotenoid profile of selected plant foods. J Chromatogr A 1218(5):684–697. doi:10.1016/j.chroma.2010.12.001
18. Garcia-de Blas E, Mateo R, Vinuela J, Alonso-Alvarez C (2011) Identification of carotenoid pigments and their fatty acid esters in an avian integument combining HPLC-DAD and LC-MS analyses. J Chromatogr B Anal Technol Biomed Life Sci 879(5–6):341–348. doi:10.1016/j.jchromb.2010.12.019
19. Gauthier-Jaques A, Bortlik K, Hau J, Fay LB (2001) Improved method to track chlorophyll degradation. J Agric Food Chem 49 (3):1117–1122
20. Bateman KP, Castro-Perez J, Wrona M, Shockcor JP, Yu K, Oballa R, Nicoll-Griffith DA (2007) MSE with mass defect filtering for in vitro and in vivo metabolite identification. Rapid Commun Mass Spectrom 21(9):1485–1496. doi:10.1002/rcm.2996
21. Castro-Perez JM, Kamphorst J, DeGroot J, Lafeber F, Goshawk J, Yu K, Shockcor JP, Vreeken RJ, Hankemeier T (2010) Comprehensive LC-MS E lipidomic analysis using a shotgun approach and its application to biomarker detection and identification in osteoarthritis patients. J Proteome Res 9(5):2377–2389. doi:10.1021/pr901094j
22. Rainville PD, Stumpf CL, Shockcor JP, Plumb RS, Nicholson JK (2007) Novel application of reversed-phase UPLC-oaTOF-MS for lipid analysis in complex biological mixtures: a new tool for lipidomics. J Proteome Res 6(2):552–558. doi:10.1021/pr060611b
23. Plumb RS, Johnson KA, Rainville P, Smith BW, Wilson ID, Castro-Perez JM, Nicholson JK (2006) UPLC/MS(E): a new approach for generating molecular fragment information for biomarker structure elucidation. Rapid Commun Mass Spectrom 20 (13):1989–1994. doi:10.1002/rcm.2550
24. Garcia-Gonzalez M, Moreno J, Manzano JC, Florencio FJ, Guerrero MG (2005) Production of *Dunaliella salina* biomass rich in 9-*cis*-beta-carotene and lutein in a closed tubular photobioreactor. J Biotechnol 115(1):81–90. doi:10.1016/j.jbiotec.2004.07.010
25. Dong L, Shion H, Davis RG, Terry-Penak B, Castro-Perez J, van Breemen RB (2010) Collision cross-section determination and tandem mass spectrometric analysis of isomeric carotenoids using electrospray ion mobility time-of-flight mass spectrometry. Anal Chem. doi:10.1021/ac101974g
26. Chauveau-Duriot B, Doreau M, Noziere P, Graulet B (2010) Simultaneous quantification of carotenoids, retinol, and tocopherols in forages, bovine plasma, and milk: validation of a novel UPLC method. Anal Bioanal Chem 397(2):777–790. doi:10.1007/s00216-010-3594-y